Jurnal Teknologi, 46(D) Jun 2007: 77–92

APPLICATION OF NEURAL NETWORK TECHNIQUE AND ELECTRODYNAMIC SENSORS IN THE IDENTIFICATION OF SOLID FLOW REGIMES

MOHD FUA'AD HJ RAHMAT[1] & HAKILO AHMED SABIT[2]

Abstract. Imaging of industrial processes have been accomplished with better efficiency and better control since the introduction of process tomography in several industries. This technique enables a deeper look into the internal conditions of a process without invading the process. In tomographic techniques, process information such as the distribution and velocity of the particles conveying at a particular plane can be obtained by placing sensors around the periphery of the plane. This paper is a continuation of a previous paper entitled Flow Regime Identification Using Neural Network-based Electrodynamic Tomography System in Jurnal Teknologi 40(D). This paper presents the results of sensors output in comparison to that of prediction models, concentration profiles and flow regimes identification obtained from the system described in the previous paper.

Keywords: Electrodynamic tomography, neural network, concentration profile, flow regimes

1.0 INTRODUCTION

The naturally occurring phenomenon of charge accumulation on dry solid particles as they convey turbulently through a pipeline forms the basic principle of electrodynamic tomography. The charges acquired by the solid particles are due to friction between the particles during flow and abrasion on the conveyor wall [1]. Mechanisms such as contact electrification, symmetric charge separation and triboelectrification are responsible for the accumulation of charge on particles flow [2]. Particles in pneumatic pipelines carry a certain amount of net electrostatic charge due to collision between particles, impact between particles and pipe wall, and friction between particles and air stream, with charge densities in the range of 10^{-7} – 10^{-3} C Kg^{-1} [3]. It is inherent that materials being pneumatically conveyed become charged [4]. Detecting and measuring the quantity of charge on the particles using an array of sensors provide information about the solids distribution in the pipe cross-section which is the main aim of tomographic systems.

Application of electrodynamic sensors for measurement of pneumatically conveying materials has been reported by several researchers. Among the early works in this

[1&2] Control and Instrumentation Department, Faculty of Electrical Engineering, Universiti Teknologi Malaysia, 81310 Skudai, Johor, Malaysia
Email: drfuaad@fke.utm.my[1], ha-sabit@lycos.com[2]

field were the design and analysis of electrodynamic transducers for velocity and mass flow rate measurement of solid particles flow [2] and investigation of multisensing of electrical charge in a cross-section, neural network based flow regimes identification, cross correlation based velocity determination and spectral analysis of electrodynamic signals [1]. Green *et al.* [6] developed an electrodynamic tomography system for a gravity conveyor. They measured particles concentration profiles and velocity profiles using discrete upstream and downstream arrays of sensors. They also applied linear back projection (LBP) method and filtered back projection (FBP) methods to reconstruct the tomograms of a particulate flow. They later combined velocity and concentration profiles to generate mass flow rate profiles in the sensing zone. Rahmat [7] analyzed linearity and frequency bandwidth of electrodynamic sensors signals and effect of electrode size on sensitivity and spatial filtering for circular and rectangular electrodes. Recently, Hezri [10] has accomplished real time velocity measurement of solid flows using upstream and downstream arrays of electrodynamic sensors. Measurements of solid particles' concentration profiles, velocity profiles and mass flow rate profiles alone do not completely satisfy economic, optimal and efficient operation of pneumatic systems. For instance, efficiency of conveying and energy consumption of pneumatic systems are determined by how the particles are distributed through the course of flow [1]. This paper proposes flow regimes identification of pneumatically conveyed solid particles utilizing neural network technique based on the solid particles charge content information obtained directly from an array of electrodynamic sensors. Resulting tomograms and sensors output are also discussed. Figure 1 shows the block diagram of the proposed tomography system.

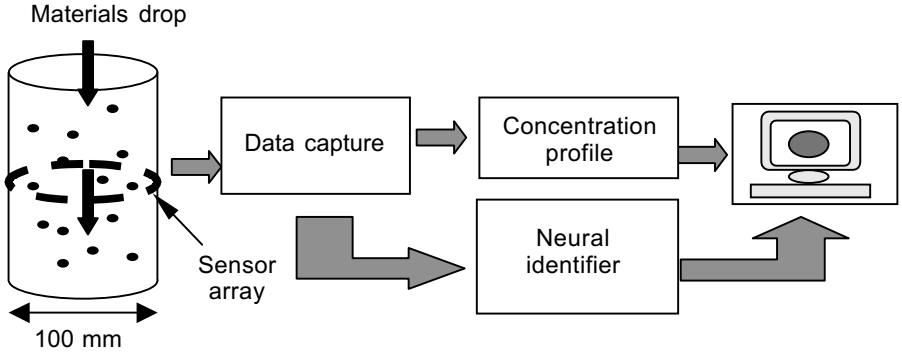

Figure 1 Block diagram of the proposed tomography system

2.0 METHODOLOGY

2.1 Data Capture

Electrodynamic sensors are used to capture information about the quantity of charge carried by the particles flowing through the conveyor at a particular plane. These are

basically passive charge to voltage converters which comprises sensing electrode and suitable charge detection circuit. The field is due to the charge on the moving solid particles and hence the name electrodynamic. The input to the sensor is through the electrode and is a physical quantity charge while the three outputs are electrical quantity. Output 1 is an AC signal used for velocity measurement, Output 2 is used for spatial filtering test and Output 3 is a DC averaged voltage output used for concentration measurement and flow regimes identification. Output 3 is the signal of interest for the proposed system highlighted below. The motivation for using electrodynamic sensors as the sensing device in tomography arises from the fact that many flowing materials pick up charge during transportation, primarily by virtue of friction of fine particles amongst themselves and abrasion on the wall of the conveyor [5]. Electrodynamic sensors are robust, of low cost and sensitive to low flow rates of dry solid materials [6]. The block diagram of an electrodynamic sensor is shown in Figure 2.

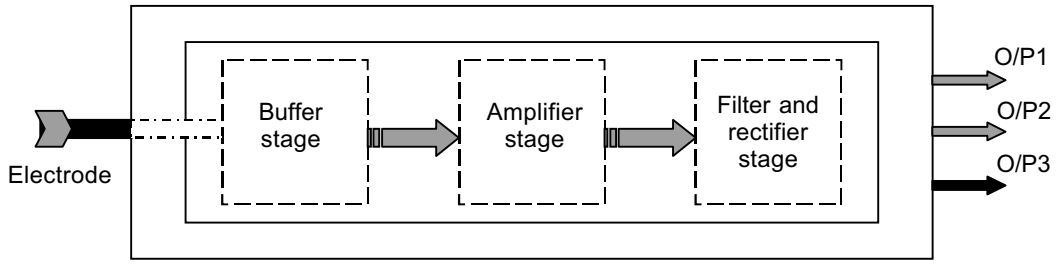

Figure 2 Block diagram of electrodynamic sensor

2.2 Data Processing

Tomographic instrumentation offers non-invasive techniques and robust sensors to solve industrial needs [7]. Flow information (i.e. charge density) captured by placing an array of 16 electrodynamic sensors are manipulated using algorithms for tomographic image reconstruction. Among the most common and simple tomographic image reconstruction algorithms are linear back projection algorithm (LBPA) and filtered back projection algorithm (FBPA). The sensors output signals are conditioned and fed into a computer to reconstruct tomographic images of the cross-section being interogated by the sensors. The tomographic images have the potential to provide information on concentration, velocity, component volume flow rate and particle size measurements [7].

2.3 Flow Regimes

The primary key to efficient design and flexible operation of many industrial manufacturing processes is high quality information concerning their actual internal states. Therefore, obtaining flow regime information certainly contributes to quality of

process information and should be considered in tomography systems. Various factors may be the cause of non-uniform particles distribution in pneumatic pipelines. The distributions of solids in a pneumatic pipeline can be highly inhomogeneous, depending upon the pipeline orientation, measurement position, phase loading, conveying air velocity and properties of the solid material including particle size, moisture content, cohesiveness and adhesiveness [3]. In this work, four types of flow regimes are created artificially by placing different shaped baffles through the pipe; full flow, three-quarter flow, half flow and quarter flow. Figure 3 shows the top view of the artificially generated flow regimes.

The flow data obtained from the artificially created flow regimes are used in training and testing a feedforward two layered back-propagation neural network to identify the four flow regimes so that the trained network can identify naturally occurring flow regimes later. This is a major step in obtaining concentration profiles for various flow regimes using filtered back projection algorithm which is of more accuracy. The back-propagation network here is trained to identify flow regimes based on direct data from the sensors rather than data available after image processing. This is to avoid time consuming image reconstruction process from delaying the identification process. The direct-from sensor data based flow regimes identification would reduce the time needed for decision-making when a control loop is involved [8]. There are 90 groups of data sets at mass flow rates ranging from 26 grm/s to 204 grm/s out of which 45 groups are used in training the network and 45 groups in testing its performance.

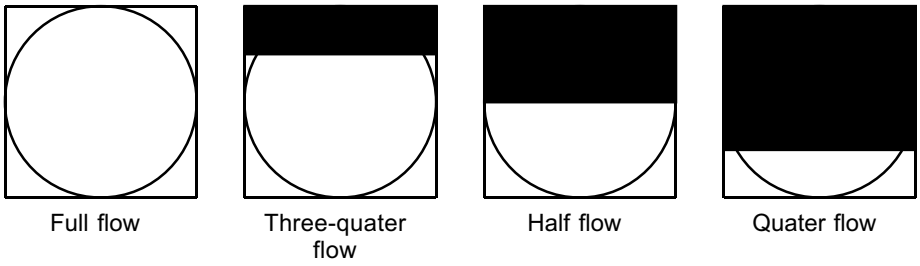

Figure 3 Top view of artificially generated flow regimes

2.4 Concentration Profiles

A concentration profile representing the solid materials distribution within the measurement plane at various mass flow rates and flow regimes is very important in the design of optimized solids flow meters. From the knowledge of material distribution and movement, internal models of the process can be derived and used as an aid for optimization of the process [9]. The concentration profiles presented in this paper are generated using Visual C++ application program developed during this project and

the flow regimes identification procedures are accomplished using a Matlab software. Concentration measurements are made using an array of sixteen electrodynamic sensors. The output from the sensors is obtained by interfacing the sensors to a personal computer (PC) via a Data Acquisition System (DAS1800). Each sensors output contains 156 samples obtained at a sampling frequency of 1 kHz. In this section, concentration measurement results and flow regimes identification results based on a neural network technique are presented.

3.0 RESULTS AND ANALYSIS

3.1 Comparison of Measured to Predicted Sensors Output

In this section, the measured average voltage output of the sensors for 10 different types of mass flow rates (26 grm/s, 45 grm/s, 65 grm/s, 85 grm/s, 105 grm/s, 125 grm/s, 145 grm/s, 165 grm/s, 184 grm/s and 204 grm/s) and 4 different flow regimes (full flow, three-quarter flow, half flow and quarter flow) are shown in Tables 1, 2, 3 and 4 along with the corresponding predicted sensors outputs. The method of calculating a scaling factor for estimating predicted output values is derived by Rahmat [7]. The above specified mass flow rates interval are chosen for convenience, however, the lowest and the highest rates are limited by the gravity flow rig hardwares.

The equation of measured outputs regression line is:

$$V_{(measured)} = 0.085 * flowrate + 19.775 \quad (1)$$

The equations of predicted outputs regression line is:

$$V_{(predicted)} = 0.085 * flowrate + 19.958 \quad (2)$$

Table 1 Measured-to-predicted outputs difference for full flow case

No.	Mass flow rate (grm/s)	Measured output (V)	Predicted output (V)	|Difference|
1	26	22.9447	23.1424	**0.1977**
2	45	24.8195	25.0448	**0.2253**
3	65	25.1991	25.4296	**0.2305**
4	85	27.3198	27.5828	**0.2630**
5	105	27.5039	27.7620	**0.2581**
6	125	27.9086	28.1656	**0.2570**
7	145	29.5724	29.8472	**0.2748**
8	165	35.0465	35.3644	**0.3179**
9	184	35.2656	35.5884	**0.3228**
10	**204**	**39.3410**	**39.6916**	**0.3506**

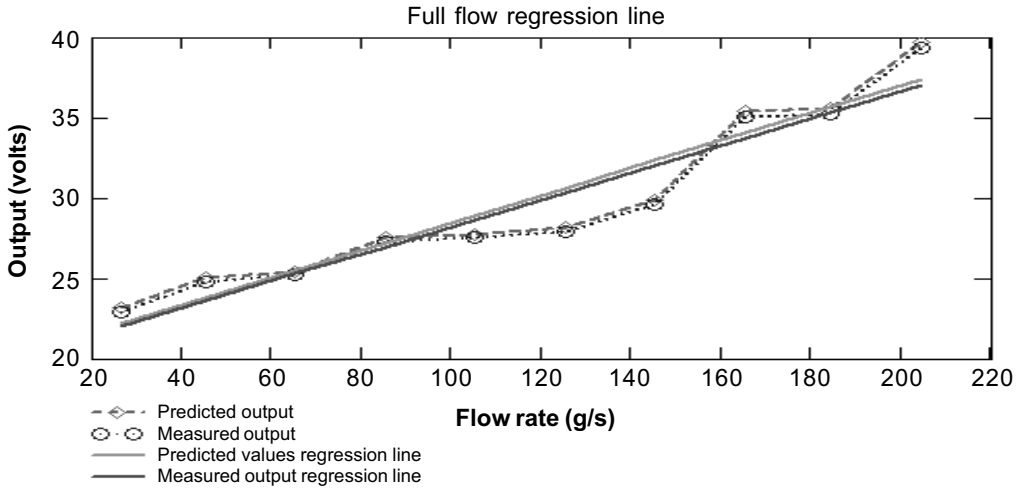

Figure 4 Sum of measured sensors output and predicted outputs along with their linear regression lines plotted against mass flow rate

Table 2 Measured-to-predicted outputs difference for three-quarter flow case

No.	Mass flow rate (grm/s)	Measured output (V)	Predicted output (V)	|Difference|
1	26	32.8559	32.8538	**0.0021**
2	45	37.5337	37.5278	**0.0059**
3	65	38.1805	38.1804	**0.0001**
4	85	38.3484	38.3523	**0.0039**
5	105	39.8649	39.8646	**0.0003**
6	125	40.5349	40.5347	**0.0002**
7	145	40.9150	40.9130	**0.0020**
8	165	41.8988	41.8921	**0.0067**
9	184	42.4663	42.4592	**0.0071**
10	**204**	**43.3965**	**43.4043**	**0.0078**

The regression lines of both measured and predicted outputs have correlation coefficient of 0.939 and the gradient of both regression lines is 0.048 hence overlapping of the regression lines is observed in Figure 5.

The equation of measured outputs regression line is:

$$V_{(measured)} = 0.048 * flowrate + 34.12 \quad (3)$$

The equation of predicted outputs regression line is:

$$V_{(predicted)} = 0.048 * flowrate + 34.117 \quad (4)$$

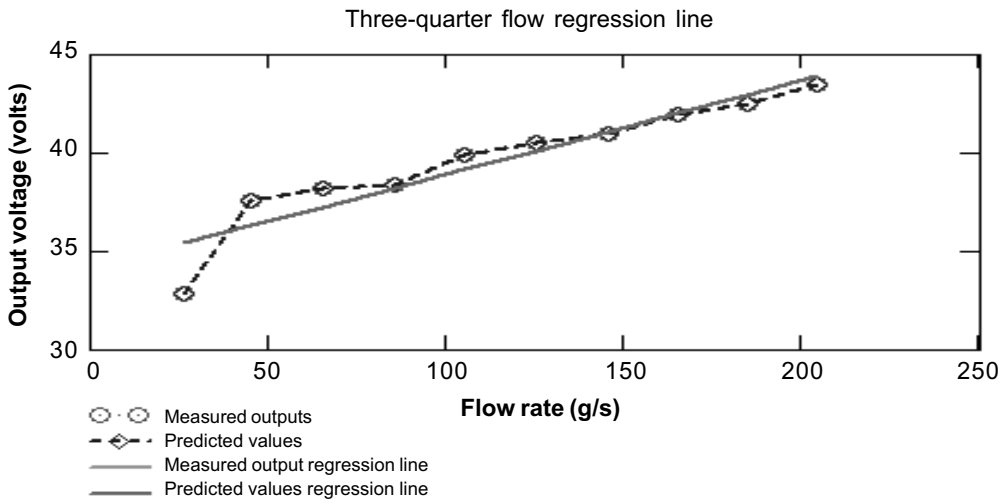

Figure 5 Sum of measured sensors output and predicted outputs along with their linear regression lines plotted against mass flow rate

Table 3 Measured-to-predicted outputs difference for half flow case

No.	Flow rate (g/s)	Measured output (V)	Predicted output (V)	|Difference|
1	26	12.7040	12.7034	**0.0006**
2	45	12.7168	12.7156	**0.0012**
3	65	15.9674	15.9586	**0.0088**
4	85	16.9735	16.9744	**0.0009**
5	105	18.5901	18.5897	**0.0004**
6	125	21.6577	21.6497	**0.0080**
7	145	28.1516	28.1477	**0.0039**
8	165	31.5338	31.5255	**0.0083**
9	184	34.1651	34.1569	**0.0082**
10	**204**	**38.0971**	**38.0855**	**0.0116**

The regression lines of both measured and predicted outputs as shown in Figure 6 have correlation coefficient of 0.978 and the gradients of both regression lines is 0.151. Therefore, the two regression lines overlap as shown in Figure 6.

The equation of measured outputs regression line is:

$$V_{(measured)} = 0.151 * flowrate + 5.753 \quad (5)$$

The equation of predicted outputs regression line is:

$$V_{(predicted)} = 0.151 * flowrate + 5.754 \quad (6)$$

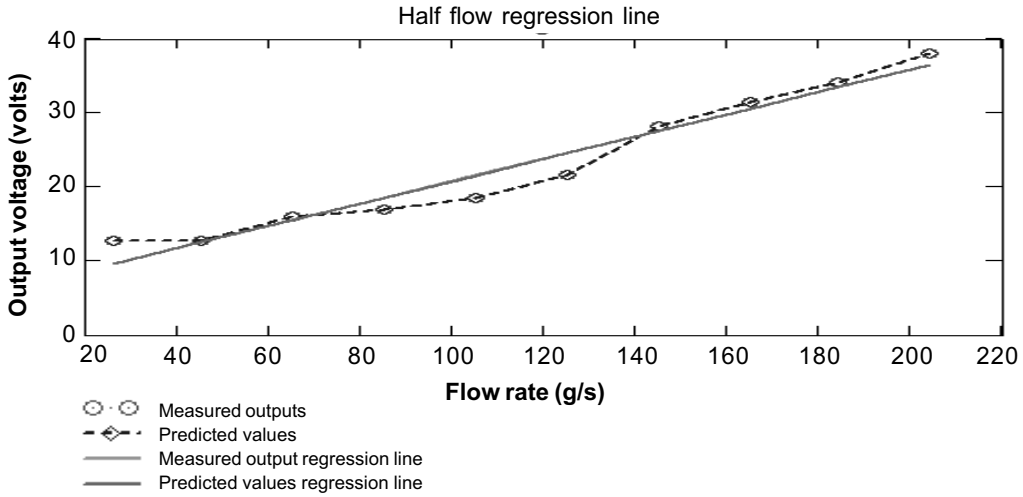

Figure 6 Sum of measured sensors output and predicted outputs along with their linear regression lines plotted against mass flow rate

Table 4 Measured-to-predicted outputs difference for quarter flow case

No.	Mass flow rate (grm/s)	Measured output (V)	Predicted output (V)	|Difference|
1	26	12.4939	16.4443	**3.9504**
2	45	13.0583	17.1892	**4.1309**
3	65	14.0137	18.4453	**4.4316**
4	85	14.0978	18.5557	**4.4579**
5	105	15.4078	20.2807	**4.8729**
6	125	15.8258	20.8331	**5.0073**
7	145	17.1155	22.5305	**5.4150**
8	165	18.2871	24.1384	**5.8513**
9	184	18.9018	24.8768	**5.9750**
10	**204**	**19.7672**	**26.0153**	**6.2481**

The equation of measured outputs regression line is:

$$V_{(measured)} = 0.042 * \ flowrate + 11.083 \tag{7}$$

The equation of predicted outputs regression line is:

$$V_{(predicted)} = 0.055 * \ flowrate + 14.584 \tag{8}$$

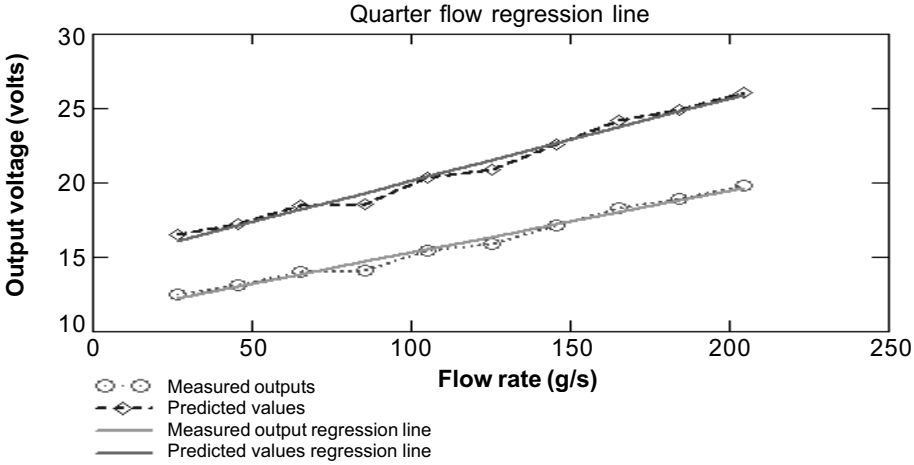

Figure 7 Sum of measured sensors output and predicted outputs along with their linear regression lines plotted against mass flow rate

3.2 Flow Regimes Identification

Results of flow regime recognition by a neural network (feed-forward back-propagation) are discussed below. The training patterns for this network are measured sensors output signals obtained by inserting various shaped baffles (Section 4, Figure 3) to artificially create different flow regimes. The training patterns represent full flow, three-quarter flow, half flow and quarter flow data at a range of flow rates. Sample training patterns are shown in Figures 8 and 9.

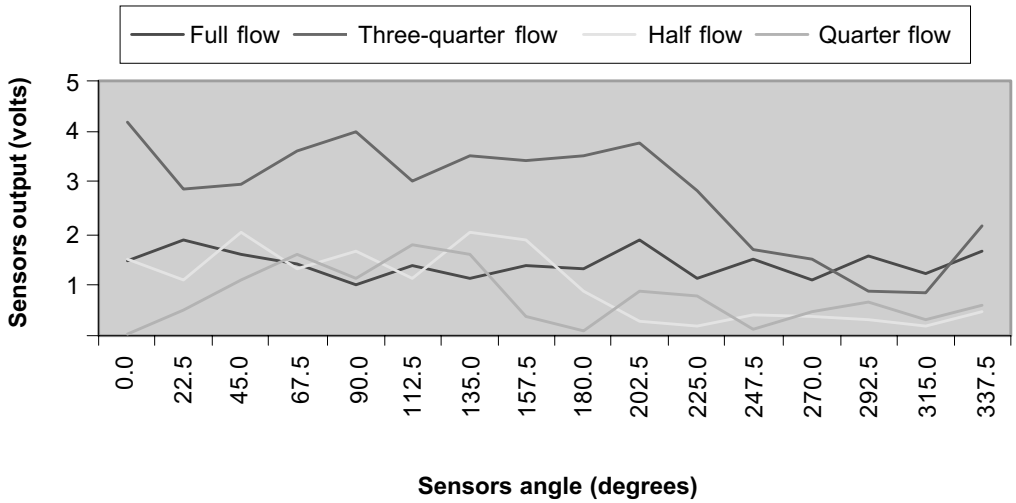

Figure 8(a) Training patterns at mass flow rate of 26 grm/s

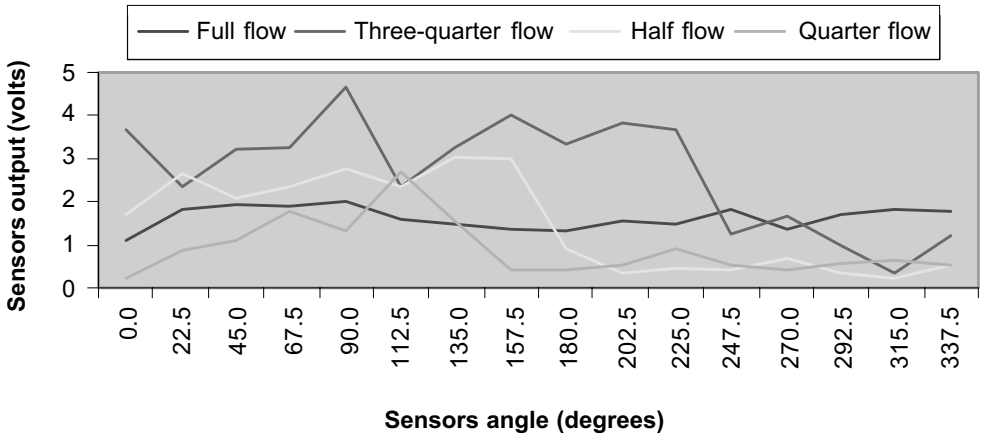

Figure 8(b) Training patterns at mass flow rate of 65 grm/s

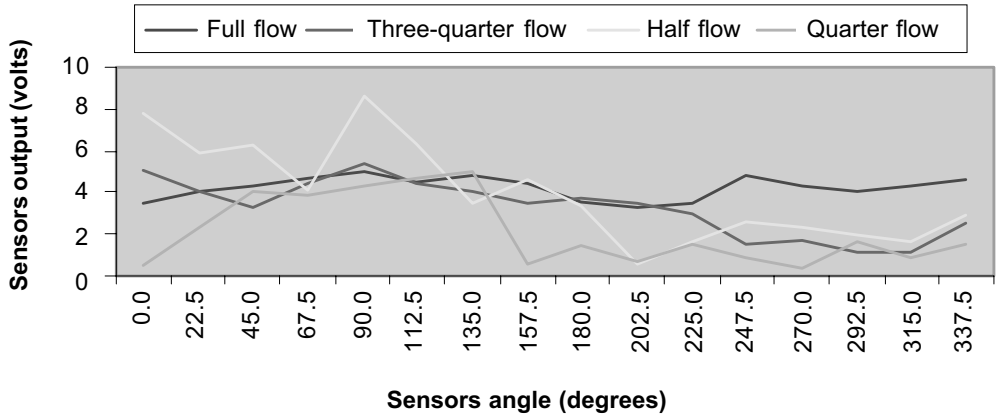

Figure 9(a) Training patterns at mass flow rate of 165 grm/s

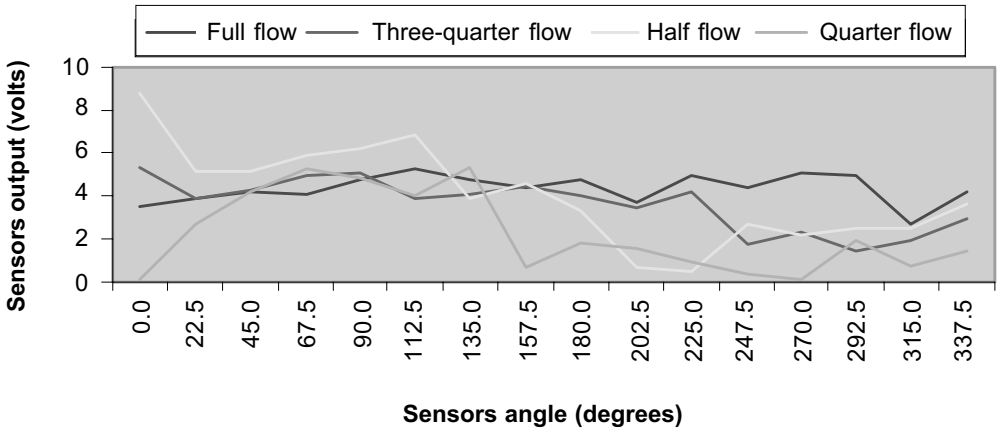

Figure 9(b) Training patterns at mass flow rate of 204 grm/s

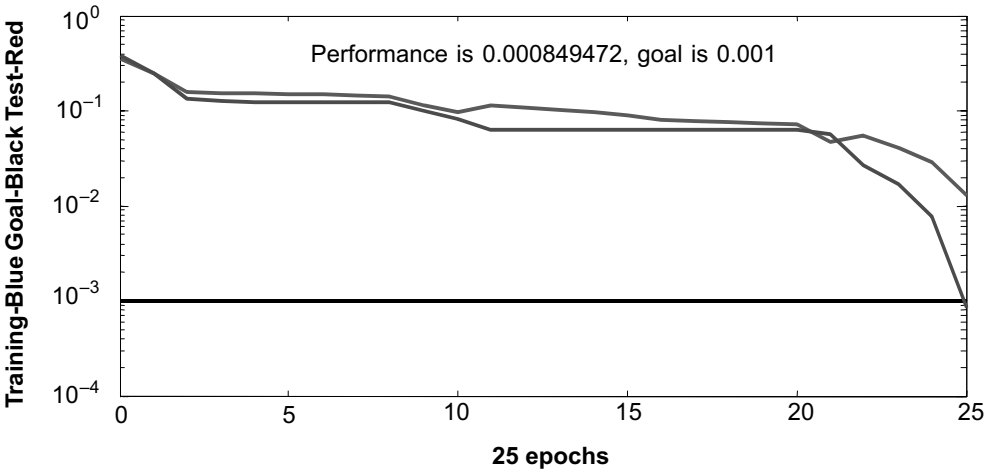

Figure 10 The performance curve of trainlm (Levenberg-Marquardt training algorithm)

Table 5 Successful identification of flow regimes

Flow regime	No. of data set	Successfull identification	Correct identification (%)
Full flow	10	9	90
Three-quarter flow	10	8	80
Half flow	10	9	90
Quarter flow	**10**	**10**	**100**

3.3 Concentration Profiles

The concentration profiles of the solid materials flow at various flow rates and flow regimes are obtained from the average outputs of electrodynamic sensors. Linear back projection and filtered back projection image reconstruction algorithms are used to obtain these profiles. All the figures in this section are generated by a Visual C++ program where darkness is related to lower solids presense.

4.0 DISCUSSION

The sums of the total voltages obtained from the experiments are closely related to the predicted values generally. However, higher voltage differences between measured and predicted values are observed in the quarter flow case which suggests that the quarter flow prediction model requires modification for better prediction.

A feed-forward back-propagation network with fast converging learning function which has been developed in a Matlab environment has been successfully used in

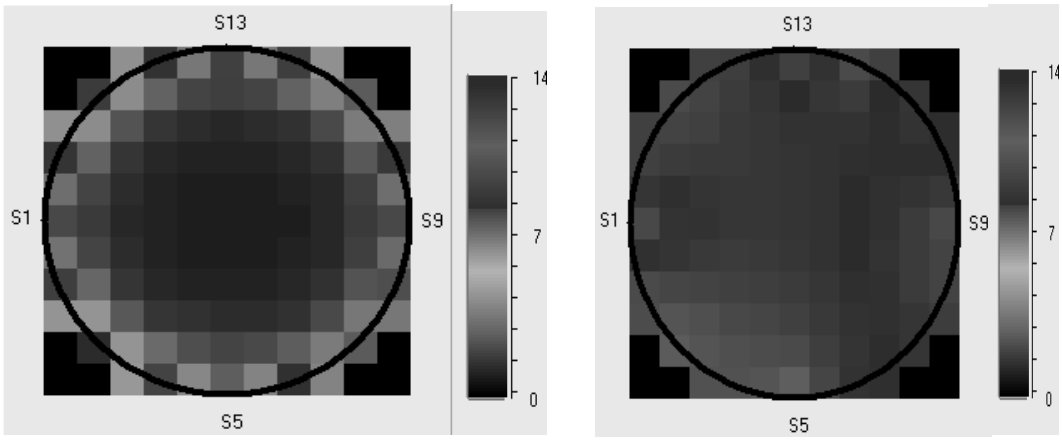

Figure 11 Concentration profiles for full flow at 45 g/s (LBPA) and (FBPA)

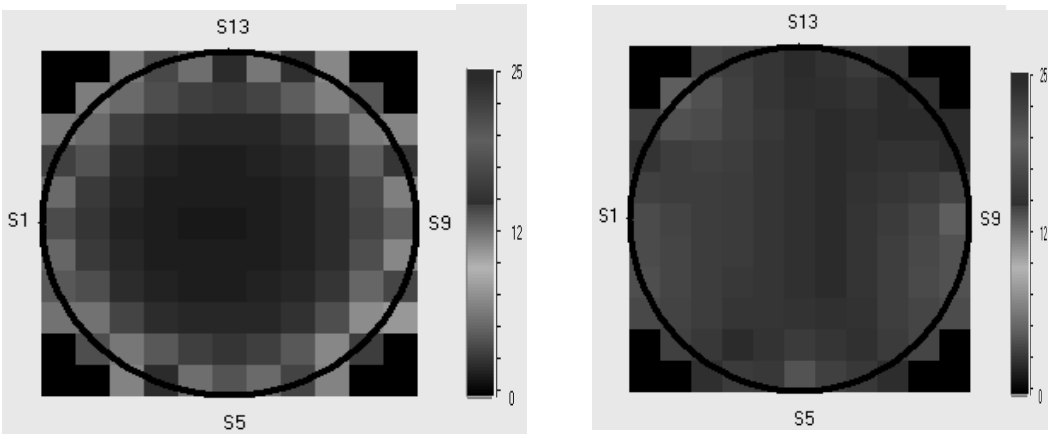

Figure 12 Concentration profiles for full flow at 125 g/s (LBPA) and (FBPA)

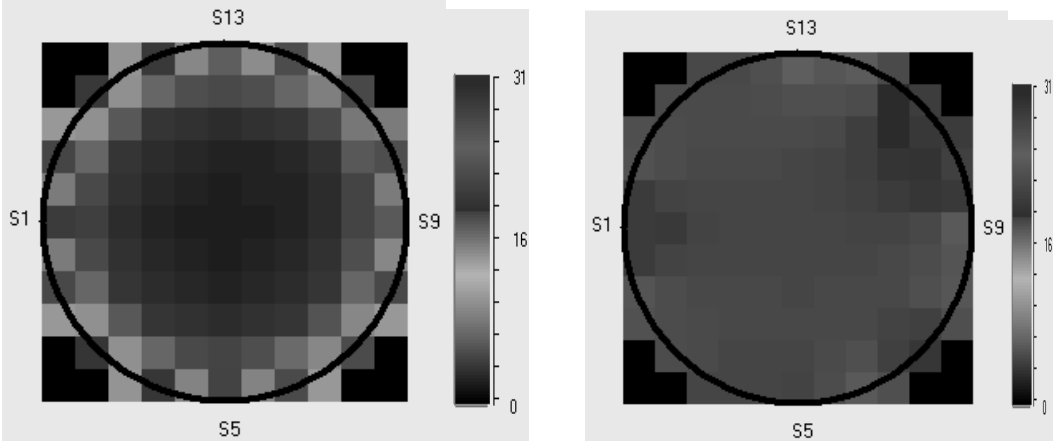

Figure 13 Concentration profiles for full flow at 165 g/s (FBPA) and (FBPA)

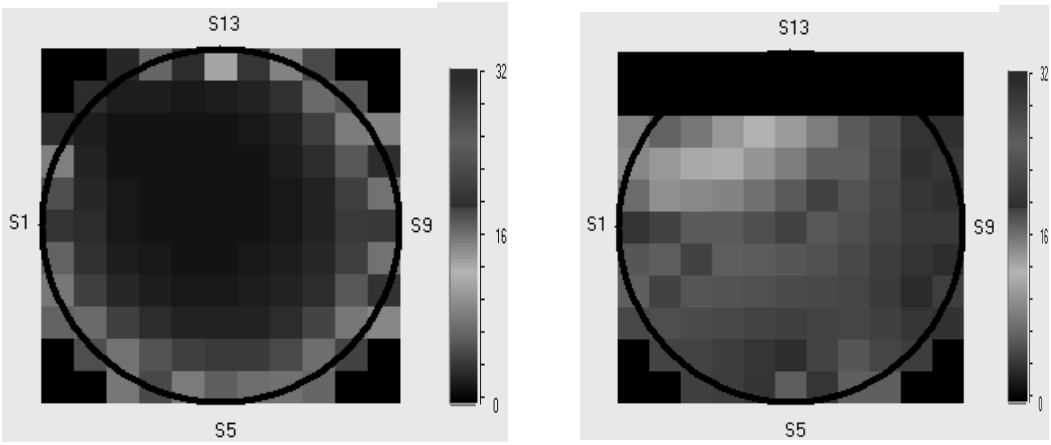

Figure 14 Concentration profiles for three-quarter flow at 45 g/s (LBPA) and (FBPA)

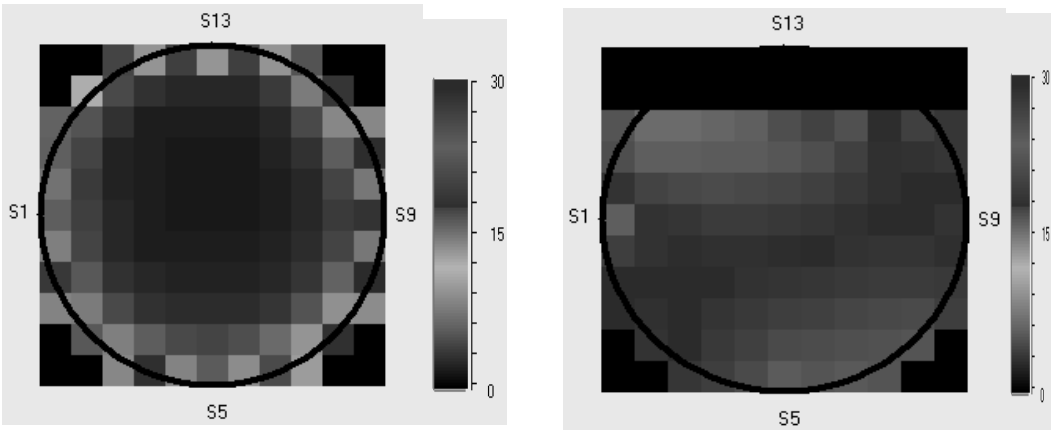

Figure 15 Concentration profiles for three-quarter flow at 125 g/s (LBPA) and (FBPA)

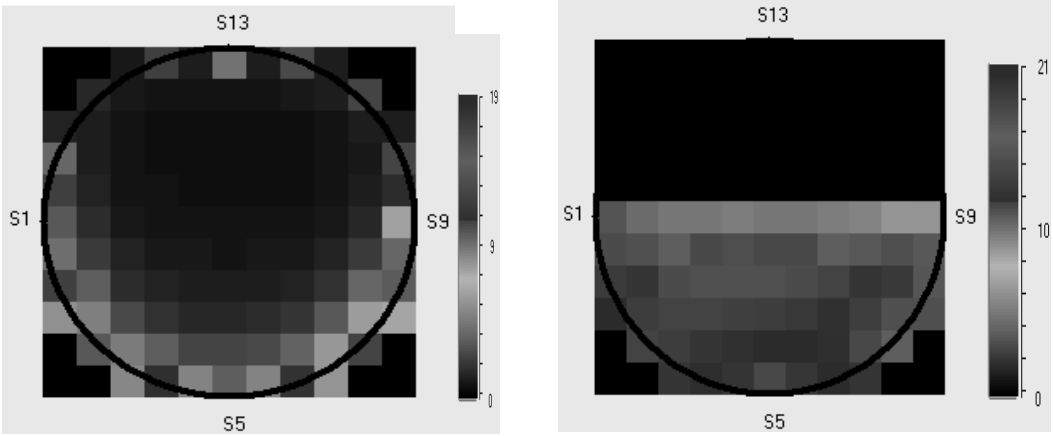

Figure 16 Concentration profiles for half flow at 45 g/s (LBPA) and (FBPA)

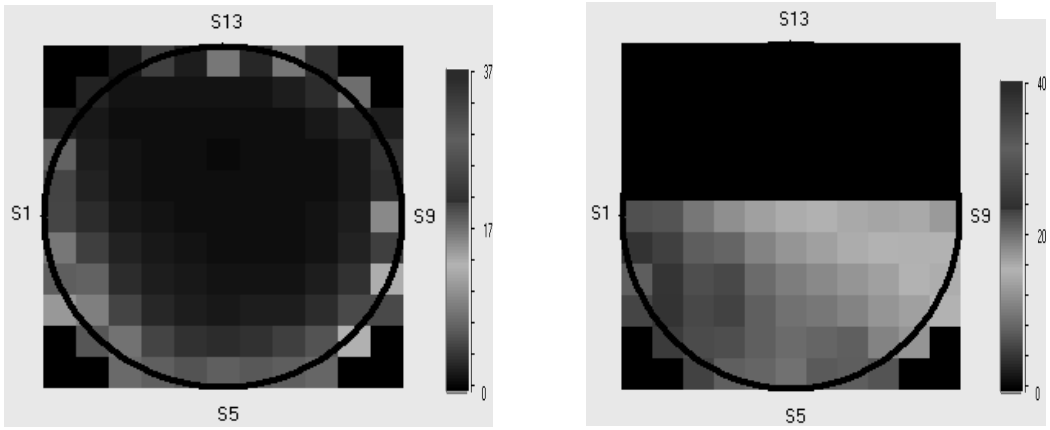

Figure 17 Concentration profiles for half flow at 125 g/s (LBPA) and (FBPA)

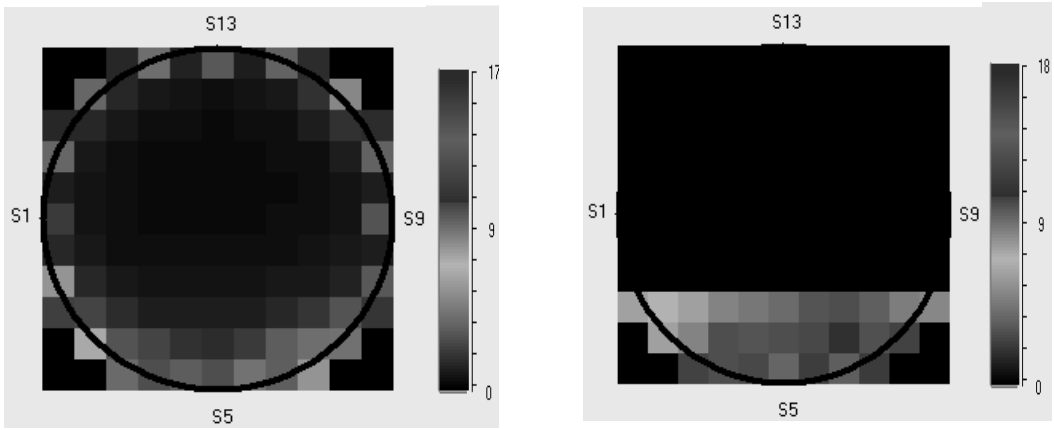

Figure 18 Concentration profiles for quarter flow at 45 g/s (LBPA) and (FBPA)

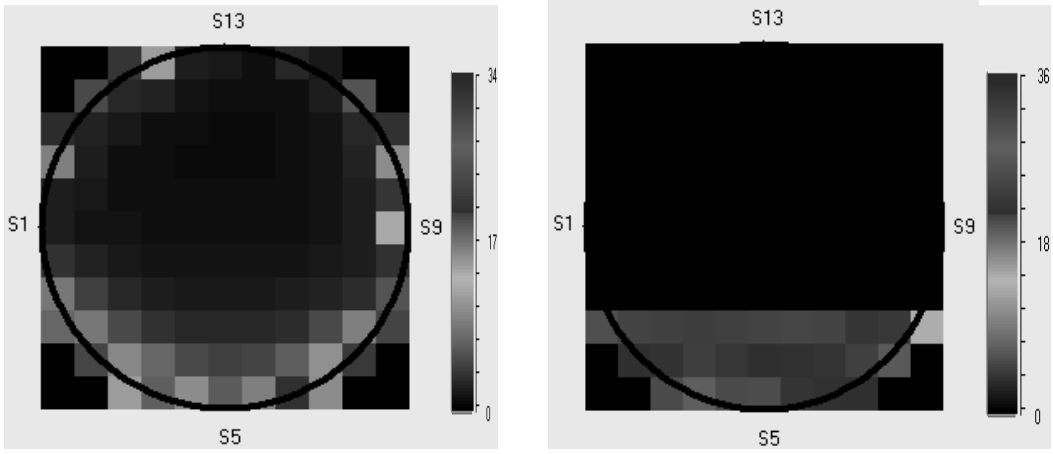

Figure 19 Concentration profiles for quarter flow at 204 g/s (LBPA) and (FBPA)

flow regime identification. The learning process of the back-propagation network is repeated for four different learning algorithms. For this particular problem, the Levenberg-Marquardt training algorithm (trainlm) is preferred as it converges in fewer number of iterations and has not been affected by overleaning which is undesirable drawback of many neural networks.

The concentration profiles of Figures 11 to 19 show the distribution of plastic bead particles at a cross-section of the conveyor pipe. For all the flow rates, the linear back projection profiles show lower pixels values towards the center of the pipe. This reveals the electrodynamic sensors' near field dominance character. However, the concentration profiles generated using filtered back projection algorithm overcame this limitation by applying filter masks to the linear back projection profiles. This is possible certainly after identifying the flow regimes using back-propagation neural network technique. Therefore, the profiles obtained from filtered back projection are more accurate representations of the particles concentration distribution.

REFERENCES

[1] Bidin, A. R. 1993. Electrodynamic Sensors and Neural Networks for Electrical Charge Tomography. Ph.D. Thesis. Sheffield Hallam University.

[2] Shackleton, M. E. 1982. Electrodynamic Transducers for Gas/Solids Flow Measurement. M. Phil Thesis. University of Bradford.

[3] Yan, Y. 1996. Mass Flow Measurement of Bulk Solids in Pneumatic Pipelines. *Meas. Sci. Technol Journal*. 7: 1687-1706.

[4] Gregory, I. A. 1987. Shot Velocity Measurement Using Electrodynamic Transducers. Ph.D. Thesis. University of Manchester Institute of Science and Technology.

[5] Cross, J. 1987. *Electrostatics; Principles, Problems & Applications*. Adam Hilger.

[6] Green, R. G., M. F. Rahmat, K. Evans, A. Goude, M. Henry, and J. A. R. Stone. 1997. Concentration Profiles of Dry Powders in a Gravity Conveyor Using an Electrodynamic Tomography System. *Meas, Sci. Technol Journal*. 8: 192-197.

[7] Rahmat, M. F. 1996. Instrumentation of Particle Conveying Using Electrical Charge Tomography. Ph.D. Thesis. Sheffield Hallam University.

[8] Yan, H., Y. H. Liu, and C. T. Liu. 2004. Identification of Flow Regimes Using Back-Propagation Networks Trained on Simulated Data Based on a Capacitance Tomography Sensor. *Meas. Sci. Technol Journal*. 15: 432-436.

[9] Azrita, A. 2002. Mass Flow Visualization of Solid Particles in Pneumatic Pipelines Using Electrodynamic Tomography System. M.E. Thesis. Universiti Teknologi Malaysia.

[10] Hezri, M. F. R. 2002. Real Time Velocity Profile Generation of Powders Conveying Using Electrical Charge Tomography. M.E. Thesis. Universiti Teknologi Malaysia.

[11] Hakilo, A. S. and M. F. Rahmat. 2004. Flow Regime Identification Using Neural Network-Based Electrodynamic Tomography System. *Jurnal Teknologi*. 40(D): 109-118.